N84-25779

ANALYSIS OF CARBON DIOXIDE BANDS NEAR 2.2 μm

M. S. Abubakar and J. H. Shaw

Department of Physics, The Ohio State University,

Columbus, OH 43210

Abstract

The absolute intensities, positions, rotational constants and half-widths of the lines of three overlapping bands of CO_2 near 4640 cm^{-1} have been determined by nonlinear, least-squares, fitting procedures. The intensities of $(00^0 2)_I \leftarrow 00^0 0$ and $(01^1 2)_I \leftarrow (01^1 0)_I$ of $^{16}O\,^{12}C\,^{18}O$ are in good agreement with the estimates in the AFGL listing. An improved value has been obtained for the intensity of $(31^1 0)_{III} \leftarrow 00^0 0$ of $^{16}O\,^{12}C\,^{16}O$.

1. INTRODUCTION

Carbon dioxide is one of the more important, atmospheric, infrared-absorbing gases due to its relatively high and increasing concentration. The spectral parameters of its bands are required for understanding radiative transfer in the atmosphere and for many other applications. In this paper, the line intensities and self-broadened widths as well as the band centers of three overlapping bands of CO_2 near 2.2 μm are reported. These were obtained by nonlinear, least-squares (NLLS) regressions based on the method of Lin et al. (1) as modified by Hoke and Shaw (2,3).

2. DATA

The experimental conditions of the CO_2 samples are summarized in Table I. The bands occur between about 4545 and 4662 cm^{-1}. Analyses of similar bands near 2600 cm^{-1} in these same spectra were reported recently (2,3) and these references give descriptions of the spectra and the calibration procedures. Because of the higher detectivity of the InSb detector at longer wavelengths the SNR of the spectra previously analyzed was in excess of 500.

Fig. 1 shows a portion of Spectrum I. The main band (centered around 4640 cm^{-1}) has no Q-branch. Because there is a weak unresolved Q-branch near 4591 cm^{-1}, the region between 4590 and 4592 cm^{-1} was assigned a weight of zero in all of the analyses. The data consisted of signal values obtained from unapodized interferograms.

3. THEORY

A spectrum similar to the observed spectrum is calculated from model functions with spectral quantities as adjustable parameters. In this analysis the models consisted of the upper and lower state energy levels, the line strengths and the dependence of the collision-broadened half-widths on rotational quantum number. The influences of the source and the observing instrument on the spectrum were also taken into consideration by modeling the effects of the retardation Δ of the interferometer mirror, the uncorrected phase error ϕ and the angular spread of the rays passing through the optical system. The frequency dependence of the baseline was described by a single parameter but, for the background, a five-degree polynomial was needed.

The calculated signal values $S'(\nu)$ are convolved with an instrument spectral response function $ISRF(\nu)$ as expressed by the relation:

$$S(\nu_j) = \int S'(\nu)\ ISRF(\nu_j,\nu)\ d\nu. \qquad [1]$$

The spectral response function used in this analysis is of the form (4),

$$ISRF(\Delta,\phi,\nu,d) = \Psi(d) \left\{ \Delta\cos\phi\ \mathrm{sinc}(2u\Delta) + \sin\phi\ \sin^2(u\Delta)/u\Delta \right\} \qquad [2]$$

where $u = \pi(\nu - \nu_o)$, and the sine and cosine functions model the uncorrected phase error ϕ. $\Psi(d)$ is a rectangular function whose half-width d depends on the angular spread of the rays passing through the interferometer. This has been described as the 'extended source effect' (4). Unlike the retardation, the phase error and extended source parameters are frequency dependent.

The line positions are given by the difference of term values

$$\nu_o(cm^{-1}) = F'(v',J',\ell') - F''(v'',J'',\ell''), \qquad [3]$$

where the primes and double primes indicate the upper and lower levels respectively. The term values are

$$F(v,J,\ell) = G_{v,\ell} + B_{v,\ell}[J(J+1) - \ell^2] - D_{v,\ell}[J(J+1) - \ell^2]^2 + \ldots , \qquad [4]$$

where the G's are the vibrational terms and the B's and D's are the rotational parameters.

Individual line intensities are expressed (5, 6), by;

$$S(m) = [8\pi^3 C_N |R(0)|^2/3hcQ_R]\ \nu_o(m)F(m)C_o(m)\ \exp[-E''(m)/kT], \qquad [5]$$

where m = -J for the P-branch and m = J + 1 for the R=branch, and

$$\left.\begin{aligned} F(m) &= (1 + \beta_1 m + \beta_2 m^2 + \ldots) \\ C_o(m) &= (m^2 - \ell^2)/|m| \end{aligned}\right\} \quad \text{for the } \pi - \pi \text{ and } \Sigma - \Sigma \text{ bands.}$$

$$\left.\begin{aligned} F(m) &= (1 + \xi m)^2 \\ C_o(m) &= |m + 1|/2 \end{aligned}\right\} \quad \text{for the } \pi - \Sigma \text{ band.}$$

C_N includes the vibrational partition sum and the natural abundance of the isotope. The other symbols have their usual meaning. This relationship yields intensities which can be compared directly with those in the AFGL Listing (7). A natural CO_2 sample was used and the isotopic abundances are assumed known.

As expected, the Lorentz and Voigt profiles yielded essentially identical results for the line widths and intensities. The |m| dependence of the widths was modeled by using the empirical relationship of Winters et al.(8).

$$\alpha(m) = \alpha_o(P,T)\left[W_o + W_1 \exp(W_2|m|) + W_3|m| \exp[-B''|m|(|m| - 1)/kT]\right] , \qquad [6]$$

where $\alpha_o(P,T) = P/P_o(T_o/T)^{1/2}$, P_o = 760 torr, T_o = 296 K, and the W_i are

regression parameters. This expression was found to be appropriate in the previous analyses (2).

The regression program compares the calculated signal values with the experimental values. The set of parameters which gives the minimum value for the sum of squares of the differences between these signal values is considered to give the best estimates for the spectral quantities. The total number of data points included in the analysis is 3883 and the number of parameters usually retrieved is between 30 and 40.

4. RESULTS

It is convenient to define a "signal-to-difference" ratio (SDR) by analogy with the signal-to-noise ratio (SNR), where the "difference" is defined as the standard deviation of the differences between the calculated and the experimental signal values. The best values of the SDR were 110 for Spectrum I and 220 for Spectrum II. The corresponding values of the SNR are 130 and 260. The differences between the SDR and SNR are primarily due to very weak lines of unmodeled hot bands.

The experimental and the calculated signal values of a portion of band I from Spectrum II are compared in Fig. 2. A plot of the residual is also shown below on an expanded scale. A 'noise spectrum' obtained from a region with no significant absorption is also given together with its corresponding residual spectrum which, in this case, is the difference from a straight line through the noise. The appearances of these two residual spectra are very similar.

a. Vibration-Rotation Constants

The vibration-rotation parameters in Table II were only determined from Spectrum I since the broader lines of Spectrum II are unsuitable for precise line-position-parameter determination. The numbers of lines modeled in each band are given in Table III. The quoted uncertainty in each parameter is 3 σ, where σ is the standard deviation estimated by the regression program. Two sets of rotational constants were obtained for band I and band II; one from a retrieval with no constraints and the other with the lower state rotational constants fixed to some recently reported values (7, 11, 12). In neither case was it possible to obtain significant estimates of the H's and these parameters have been assigned the value zero.

The band centers in Table II include the contribution due to the vibrational angular momentum quantum number, so that

$$\nu_{center} = \Delta G_{v',v''} + (B''\ell''^2 + D''\ell''^4 - B'\ell'^2 - D'\ell'^4) , \qquad [7]$$

where $\Delta G_{v',v''}$ is the difference between the upper and lower vibrational levels. Other estimates of band parameters are also included in Table II.

Different estimates for the relative line positions for band I are compared in Fig. 3. The differences are given by $\nu_a - \nu_r$ where the ν_r are the line positions calculated with the constants obtained from the best unconstrained retrieval and ν_a are the positions obtained by assuming a common band center and either the parameters reported by other investigators or obtained from other retrievals assuming a common band center. The three unlabeled curves near the zero line represent parameters from three different unconstrained retrievals with essentially the same SDR values. Their

agreement is a measure of the internal consistency of the results. Line position differences for the other bands are less consistent since the bands are weaker and hence their parameter estimates are less precise than those of band I.

The rotational parameters from Spectrum I were used to calculate the line positions of Spectrum II but new values for the band centers of Spectrum II were retrieved. These showed a shift of about 0.01 cm^{-1} from the low pressure positions. Shifts of this magnitude are within the range routinely observed on spectra measured on different days with our equipment. They are attributed to small changes in the optical alignment of the spectrometer (2) and they make it necessary to calibrate each spectrum individually (13).

b. Intensities

The band intensity is the sum of the line intensities $S_i(\nu)$:

$$S^\circ = \sum_{i=1}^{\infty} S_i(\nu) ,$$

The dipole moment matrix elements and band intensities obtained from both spectra are given in Table IV. A strong Coriolis interaction in band II causes the intensity asymmetry of the P- and R-branches shown in Fig. 4. Line intensities for this band vanish near m = -6. The existence of similar asymmetries in other $\pi - \Sigma$ bands of CO_2 has also been reported (14, 15, 16, 17). The subbands of band III were treated as separate bands with a common band center and dipole moment. The reported band intensity is the sum of the intensities of both sets of lines. It was found that vibration-rotation

interaction parameters could only be retrieved for band II.

c. Half-widths

The Lorentz widths as functions of |m| shown in Fig. 5 were obtained from the parameter values of Table V. There is good agreement for |m| > 10. The same width parameters were used for all bands in each spectrum. In Fig. 6 the widths from the high pressure spectrum are compared with values obtained from the 2600 cm^{-1} region of the same spectrum and from near 2760 cm^{-1} in another spectrum recorded at 741 torr and 292 K (2, 18). There is some evidence of a weak dependence of the widths on the vibrational transition although the differences between the previously estimated widths and those reported in this work are within 3 σ, where σ is the standard deviation in $\alpha(m)$ estimated from the standard deviations of the parameters W_i of Eq. (6).

d. On background, baseline and instrument effects

A five-degree polynomial was required to model the background. The baseline was more difficult to determine because of the small absorptances of the lines (average peak absorptance value ~0.25). For Spectrum II a value of -0.100(2) was found. This is about 10% of the observed signal for zero absorptance. In Spectrum I the retrieved value of the baseline shift was smaller than its uncertainty and hence it was set to zero. The retrieved values for the retardation shown in Table VI agree with those estimated previously (4).

5. DISCUSSION

Despite the decreased SNR the overall precision obtained in the determination of intensities and rotational constants is comparable with that reported for the 2600 - 2800 cm^{-1} region in the previous analyses. As expected, the most precise constants and intensities were obtained from the strongest band (band I). The intensity of band II appears to be significantly greater than the estimate given in the AFGL listing (7). We are not aware of any other reported experimental values for these band intensities.

The dipole moment matrix element values in Table IV agree within 1% for band I and 2% for band II and band III. This is within the estimated experimental errors.

It appears, from Table V, that, although there is some uncertainty in the width parameters, the CO_2 widths from different spectral regions and different spectra are essentially consistent within the experimental uncertainty.

References

1. C. L. Lin, J. H. Shaw and J. G. Calvert, "Band Analysis by Spectral Curve Fitting," J. Quant. Spectrosc. Radiat. Transfer, 23, 387 (1980).

2. M. L. Hoke and J. H. Shaw, "Analysis of CO_2 bands near 2600 cm^{-1}," Appl. Opt. 21, 929 (1982).

3. M. L. Hoke and J. H. Shaw, "Rotational Analysis of CO_2 Bands near 4 μm," Appl. Opt. 21, 935 (1982).

4. M. L. Hoke, "Analysis of CO_2 Bands near 2600 cm^{-1}," Ph.D. Dissertation, Ohio State University (1982).

5. S. S. Penner, "Quantitative Molecular Spectroscopy and Gas Emissivities," Addison-Wesley Reading, Mass (1959).

6. C. P. Rinsland, A. Baldacci and K. N. Rao, "Strengths of $^{13}C^{16}O_2$ Lines at 4.3 μm," J. Molec. Spectrosc. 81, 256 (1980).

7. L. S. Rothman and L. D. G. Young, "Infrared Energy Levels and Intensities of Carbon Dioxide," J. Quant. Spectrosc. Radiat. Transfer, 25, 505 (1981).

8. B. H. Winters, S. Silverman and W. S. Benedict," Line Shape in the Wing beyond the Band Head of the 4.3 μm Band of CO_2," J. Quant. Spectrosc. Radiat. Transfer, 4, 527 (1964).

9. J. Y. Mandin, "Interpretation of the CO_2 Absorption Bands Observed in the Venus Spectrum between 1 and 2.5 μm," J. Molec. Spectrosc. 67, 304 (1977).

10. A. Chedin, "The Carbon Dioxide Molecule: Potential, Spectroscopic, and Molecular Constants from its Infrared Spectrum," J. Molec. Spectrosc. 76, 430 (1979).

11. G. Guelachvili, "High-Resolution Fourier Spectra of Carbon Dioxide and Three of its Isotopic Species near 4.3 μm," J. Molec. Spectrosc. 79, 72 (1980).

12. H. Sakai, "Molecular Constants of $^{12}C^{16}O_2$ Bands in 1900 cm^{-1} ~2150 cm^{-1}," Paper ME7, 38th Symposium on Molecular Spectroscopy, Ohio State University, Columbus, OH 43210 (1983).

13. R. L. Hawkins, M. L. Hoke, and J. H. Shaw, "Wavenumber Calibration of Fourier Transform Spectra," Appl. Spectrosc. 37, 134 (1983).

14. Ph. Arcas, E. Arié, Ph. Cardinet, A. Valentin, and A. Henry, "Intensity of CO_2 Bands in the 4.8- to 5.3-μm Region. The $(11^10, 03^10)_{II} \leftarrow 00^00$ Band," J. Molec. Spectrosc. 81, 262 (1980).

15. C. P. Rinsland, D. C. Benner, D. J. Richardson, and R. A. Toth, "Absolute Intensity Measurements of the $(11^10)_{II} \leftarrow 00°0$ band of $^{12}C^{16}O_2$ at 5.2 μm," Appl. Opt. 22, 3805 (1983).

16. H. D. Downing, B. J. Krohn, and R. H. Hunt, "Coriolis Intensity Perturbations in $\pi - \Sigma$ Bands of CO_2," J. Molec. Spectrosc. 55, 66 (1975).

17. Ph. Arcas, E. Arié , A. Valentin, and A. Henry, "Intensity of CO_2 Bands in the 4.8 - 5.3 μm Region. The $(11^10, 03^10)_I \leftarrow 00°0$ Band," J. Molec. Spectrosc. 96, 288 (1982).

18. M. L. Hoke and J. H. Shaw, "Parameters of CO_2 Bands near 3.6 μm," Appl. Opt. 22, 328 (1983).

Table I

Experimental conditions of the CO_2 samples analyzed.

Condition	Spectrum I	Spectrum II
Pressure (torr)	177	658.5
Temperature (K)	294.2	294.2
Pathlength (m)	476	131
SNR	~130	~260

Table II

Retrieved rotational constants compared with other reported values. The letters at the end of rows identify the constants according to the following assignments; M: Mandin (Ref. 9), C: Chedin (Ref. 10), R: AFGL listing (Ref. 7), F: Lower state rotational constants fixed to the values reported by Guelachvili (Ref. 11) for band I, by Sakai (Ref. 12) for band II and by AFGL (Ref. 7) for band III. The upper state constants are retrieved, U: Constants retrieved with no constraints.

The figures in parentheses are the uncertainty in the last digits.

TABLE II

Band	Isotope	Transition	Band Center	B'	B''	D' x 10^7	D'' x 10^7	
I	$^{16}O^{12}C^{18}O$	$(00^02)_I \leftarrow 00^00$	4639.5081(8)	0.3623911(27)	0.3681879(17)	1.146 (36)	1.170 (29)	U
			4639.5082(3)	0.3623894(14)	0.36818571	1.1693 (93)	1.19030	F
			4639.502	0.362372	0.3681771	1.11	1.17	R
			4639.512	0.362384	0.368186	1.18	1.19	C
			4639.5031	0.36239118	0.3681834	1.1967	1.1800	M
II	$^{16}O^{12}C^{16}O$	$(31^10)_{III} \leftarrow 00^00$	4591.1192(28)	0.38996(22)	0.39025(26)	1.52 (14)	1.30 (72)	U
			4591.1195(28)	0.389939(28)	0.39021894	1.585 (99)	1.33281	F
			4591.118	0.389925	0.39021894	1.53	1.33373	R
			4591.027	0.389927	0.390221	1.54	1.33	C
			4591.1188	0.38992250	0.3902215	1.5284	1.3373	M
III_c	$^{16}O^{12}C^{18}O$	$(01^12)_I \leftarrow (01^10)_I$	4614.7792(60)	0.362857(54)	0.3685824	1.27 (60)	1.14	F
			4614.780	0.362848	0.3685824	1.06	1.14	R
			4614.787	0.362849	0.368604	1.19	1.20	C
			4614.7794	0.3628716	0.3685996	1.2561	1.1302	M
III_d	$^{16}O^{12}C^{18}O$	$(01^12)_I \leftarrow (01^10)_I$	4614.7792(60)	0.363414(36)	0.3691366	1.41 (48)	1.14	F
			4614.780	0.363356	0.3691366	1.06	1.14	R
			4614.787	0.363376	0.369156	1.20	1.21	C
			4614.7808	0.36339483	0.3691715	1.2033	1.2559	M

Table III

Number of P and R lines which can be distinguished above the noise level and analyzed for each band.

Band	Number of P lines	Number of R lines
I	57	49
II	26	30
III c	34	34
III d	34	34

Table IV (a)

Rotationless Dipole Moment Matrix Elements

Band	$\|R(0)\| \times 10^5$ Debye	
	Spectrum I	Spectrum II
I	136 (1)	137 (1)
II	1.21 (9)	1.19 (3)
III	147 (4)	149 (4)

Table IV (b)

Band intensities compared with the AFGL listing (Ref. 7)

Band	$S^0 \times 10^{22}$ (cm^{-1}/mol-cm^{-2})		
	Spectrum I	Spectrum II	AFGL
$^{16}O^{12}C^{18}O$ $00^02 \leftarrow 00^00$	0.122 (1)	0.124 (2)	0.1302
$^{16}O^{12}C^{16}O$ $(31^10)_{III} \leftarrow 00^00$	0.019 (6) $\xi = 0.164$ (4)	0.019 (2) $\xi = 0.168$ (2)	0.00205 $\xi = 0.18$
$^{16}O^{12}C^{18}O$ $(01^12)_I \leftarrow (01^10)_I$	0.0108 (5)	0.0111 (6)	0.01042

Table V

Self-broadened Lorentz width parameters

for one atmosphere, 296 K.

Parameter	Spectrum		Hoke and Shaw (Ref. 18)	
W_i	I	II	2614 cm^{-1}	2757 cm^{-1}
$W_o \times 10^2$ cm^{-1}	8.2 (2)	8.34 (9)	8.34 (2)	8.0732 (8)
$W_1 \times 10^2$ cm^{-1}	4.8 (1.0)	6.8 (2)	5.83 (6)	6.15 (4)
W_2	-0.15 (4)	-0.171 (9)	-0.1539 (4)	-0.179 (9)
$W_3 \times 10^3$ cm^{-1}	3.3 (3)	3.1 (1)	1.82 (2)	1.89 (9)

Table VI

Values of maximum optical path difference (retardation) obtained by various analyses.

REF	Retardation (cm)	
	Spectrum	
	I	II
Hoke (Ref. 4)	16.51 (10)	16.64 (10)
This work	16.48 (15)	16.47 (9)

Figure Captions

Fig. 1

The portion of Spectrum I analyzed. Lines of the bands centered at 4639.5 cm^{-1} and 4591.1 cm^{-1} are easily identified but lines of the much weaker band, centered at 4614.8 cm^{-1}, can hardly be distinguished above the noise.

Fig 2.

Corresponding portions of the residual spectrum and the noise spectrum are shown. The upper spectrum is the part of the experimental spectrum shifted by 0.2 units with respect to the calculated spectrum.

Fig. 3

Comparison of line position differences. Differences are plotted against rotational index m. The letters labeling the plots are the same as those used in Table II.

Fig. 4

Calculated intensities of the lines of band $(31^{1}0)_{III} \leftarrow 00^{0}0$ of $^{16}O^{12}C^{16}O$ plotted against rotational index m.

Fig. 5

The |m| dependence of the line widths for Spectrum I and Spectrum II. All widths have been reduced to 296 K and 760 torr.

Fig 6

Comparison of the |m| dependence of the widths of lines of Spectrum II with other results from (Ref. 18). All widths reduced to 296 K and 760 torr.

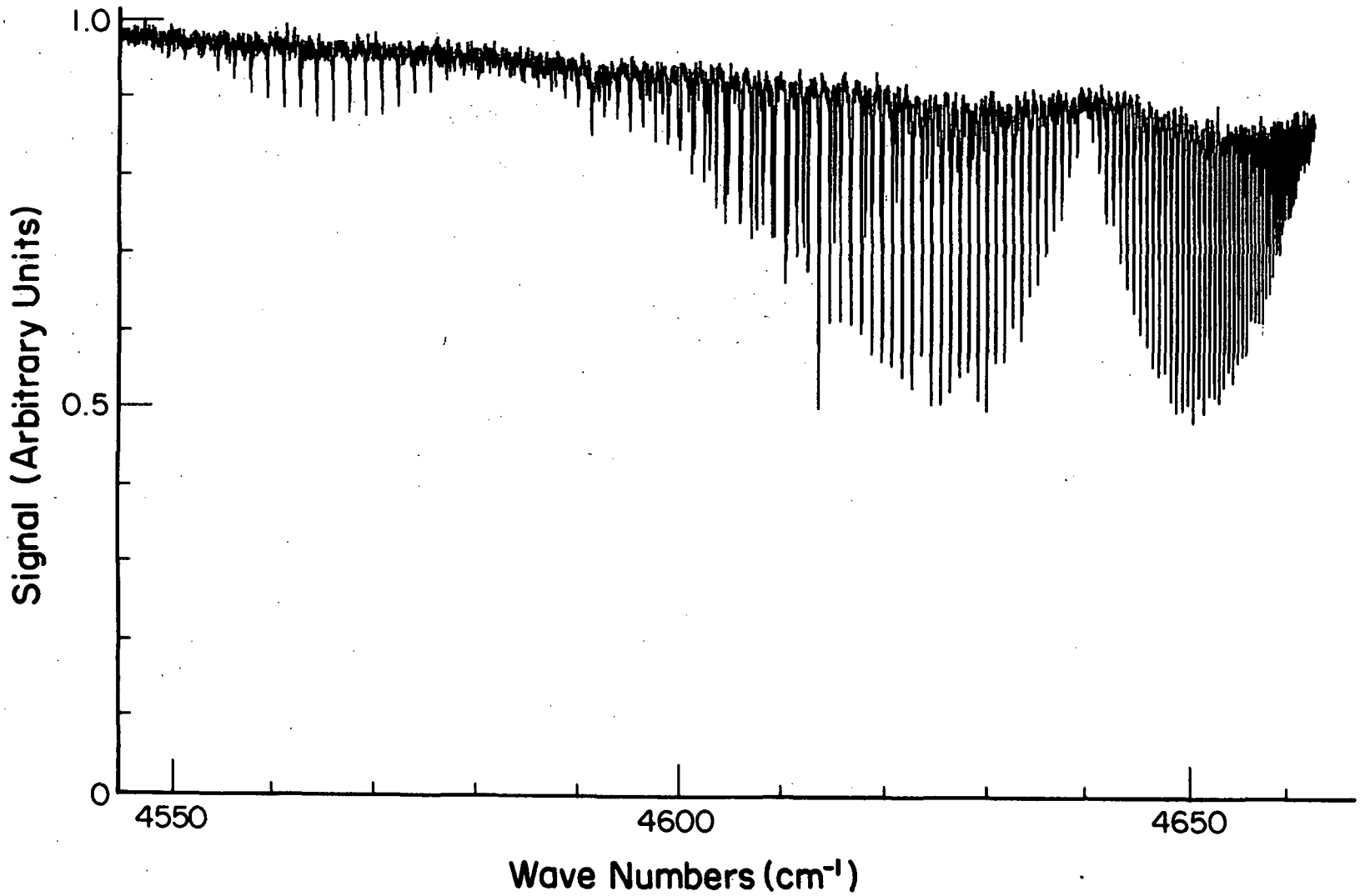
1.0
0.5
0
Signal (Arbitrary Units)
4550
4600
4650
Wave Numbers (cm⁻¹)

Fig. 1

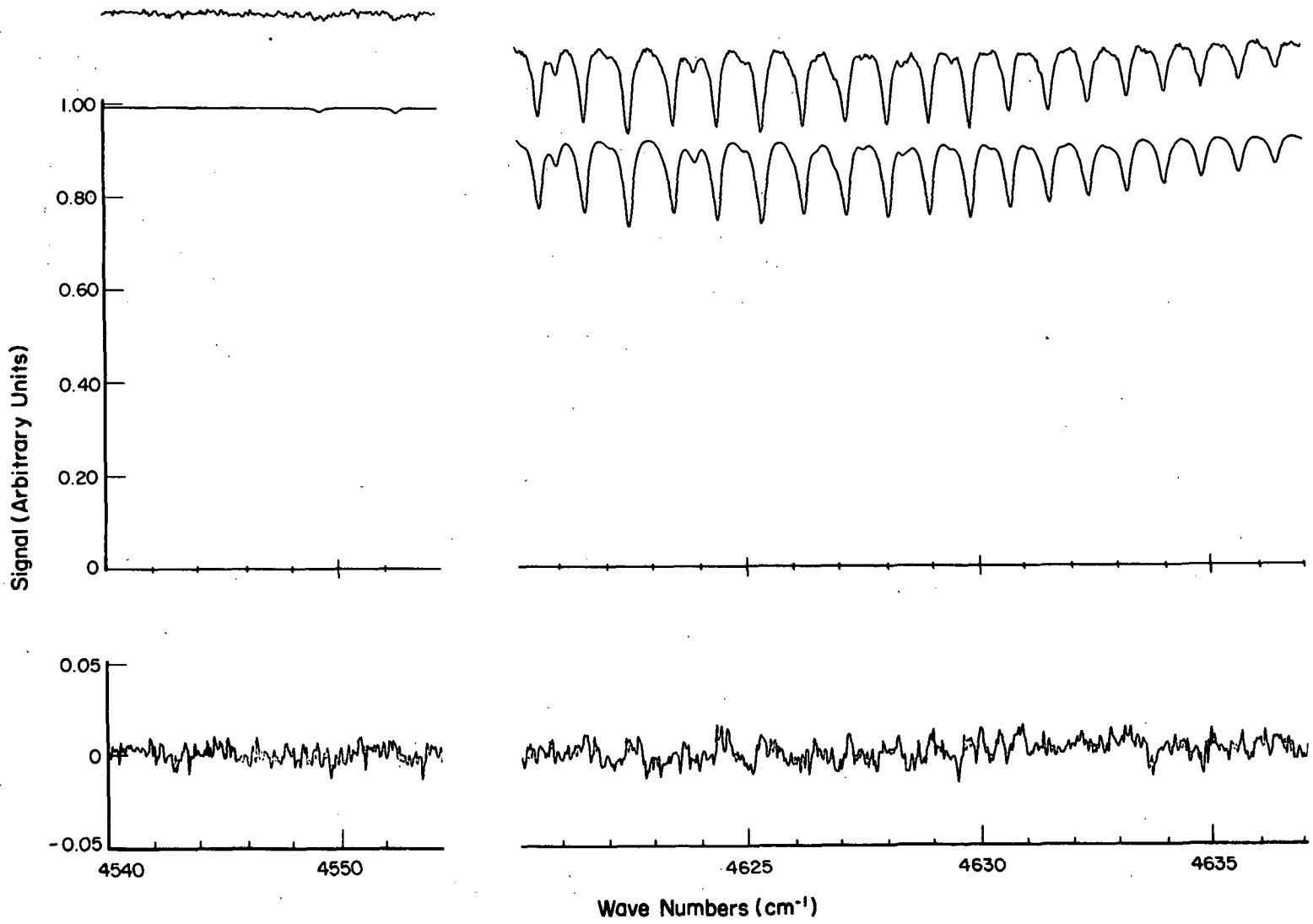
1.00
0.80
0.60
0.40
0.20
0
Signal (Arbitrary Units)
0.05
0
-0.05
4540
4550
4625
4630
4635
Wave Numbers (cm⁻¹)

F.5. 2

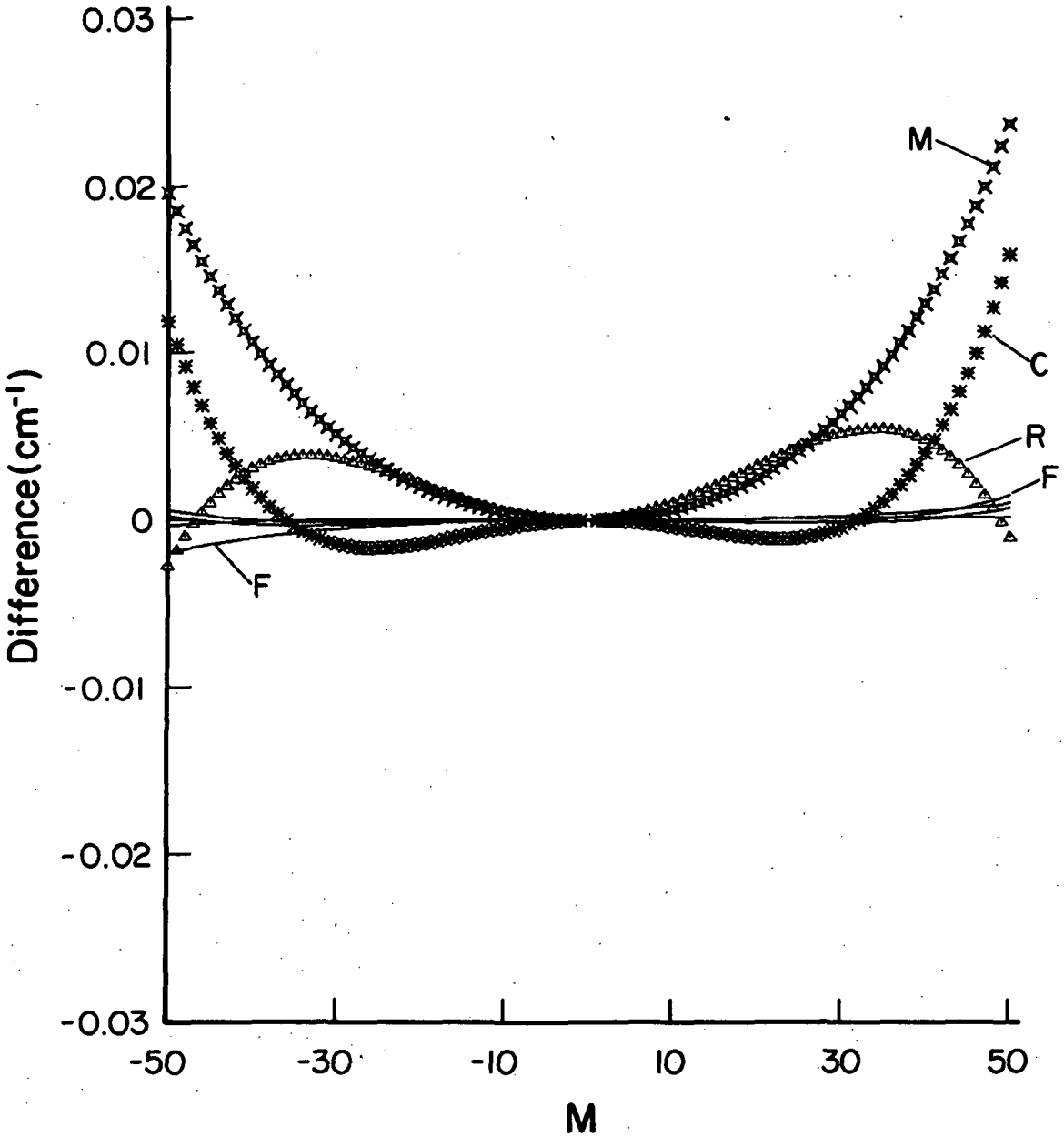
0.03
0.02
0.01
0
-0.01
-0.02
-0.03
Difference(cm⁻¹)
-50
-30
-10
10
30
50
M
M
C
R
F
F

Fig. 3

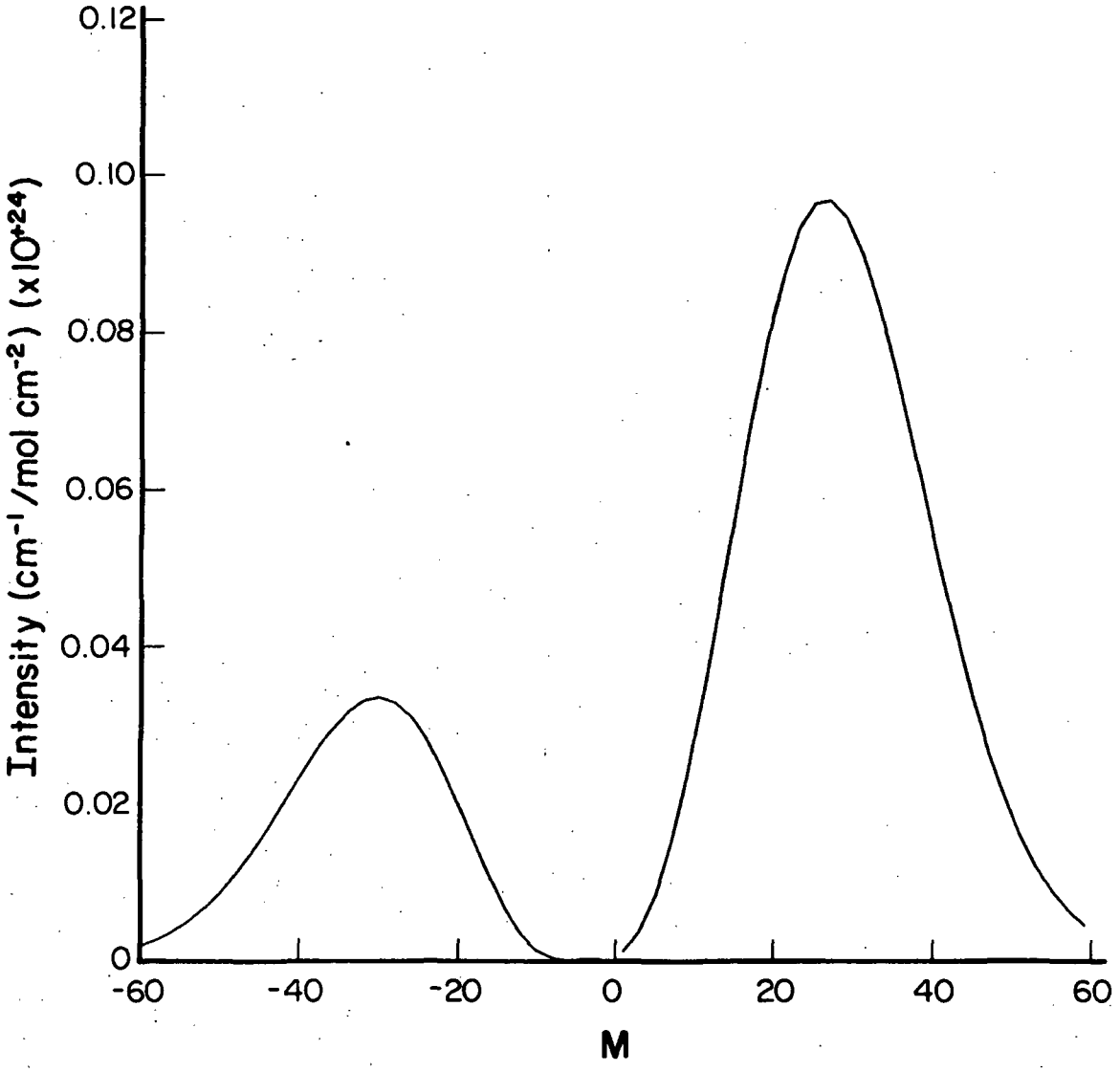
0.12
0.10
0.08
0.06
0.04
0.02
0
Intensity (cm⁻¹/mol cm⁻²) (x10*24)
-60
-40
-20
0
20
40
60
M

Fig. 4

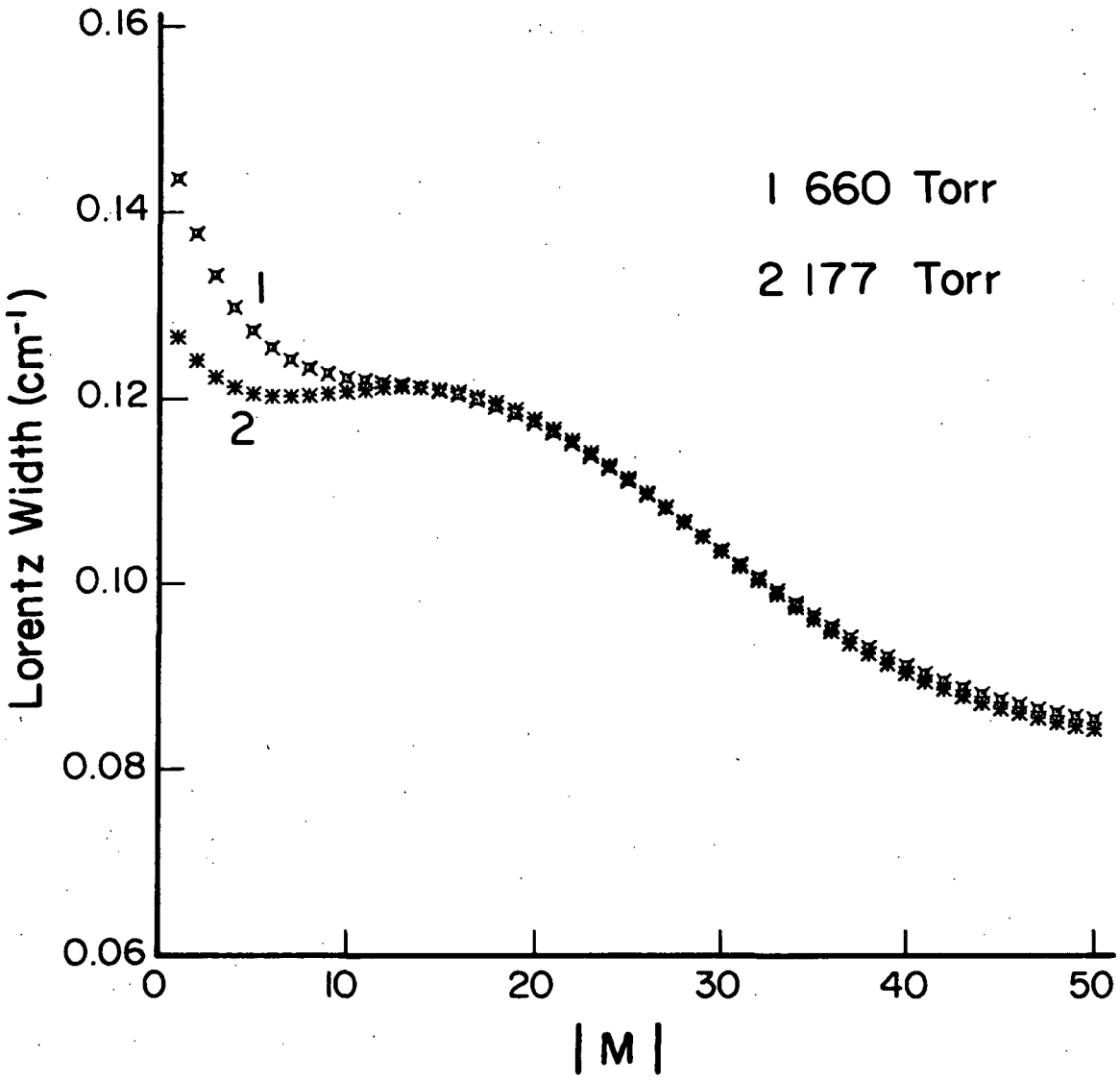
0.16
0.14
0.12
0.10
0.08
0.06
Lorentz Width (cm⁻¹)
1 660 Torr
2 177 Torr
1
2
0
10
20
30
40
50
| M |

Fig. 5

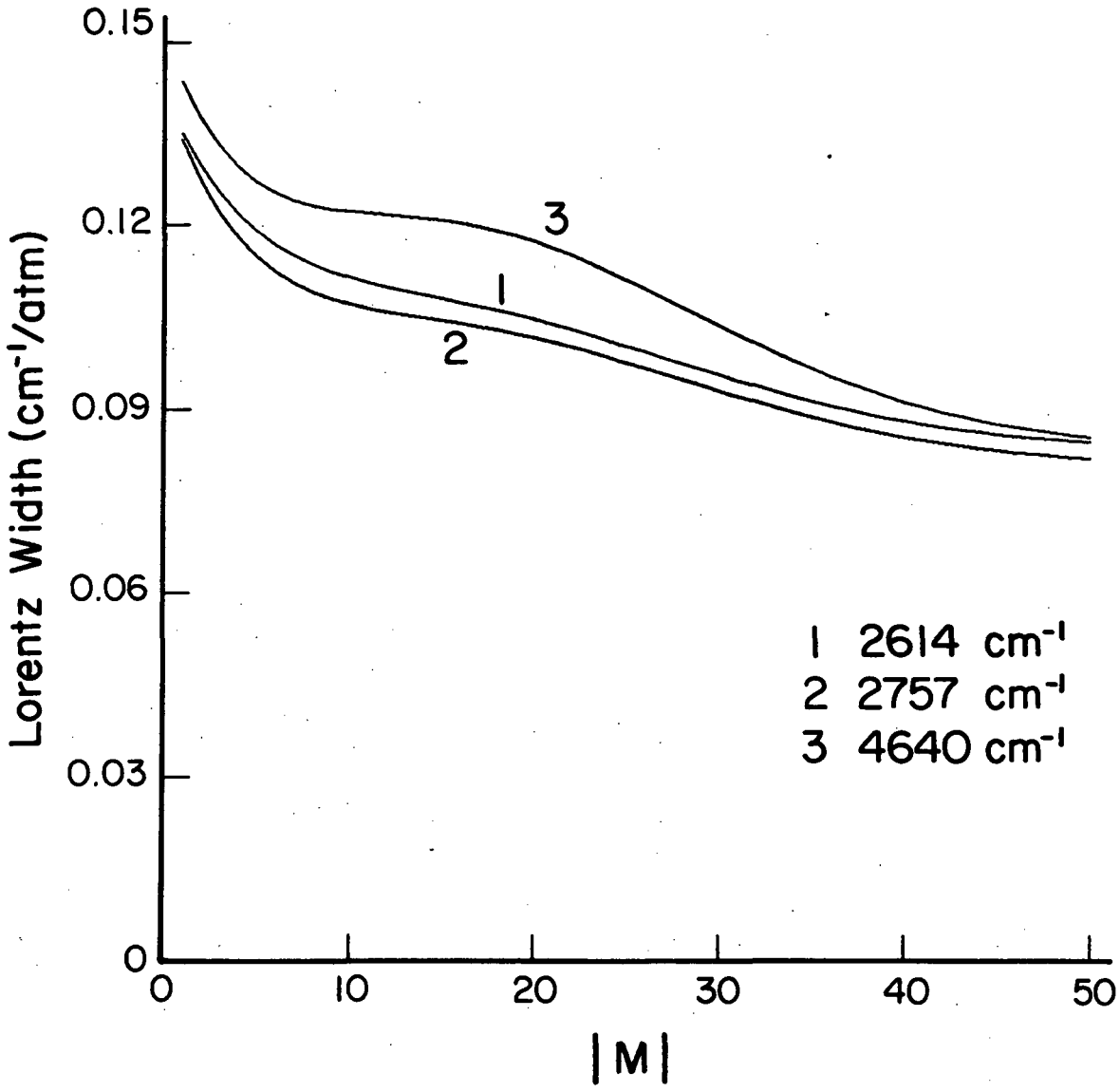
0.15
0.12
0.09
0.06
0.03
0
Lorentz Width (cm⁻¹/atm)
0
10
20
30
40
50
|M|
1
2
3
1 2614 cm⁻¹
2 2757 cm⁻¹
3 4640 cm⁻¹

Fig. 6